transmitter consists of a planar antenna (slot antenna) chip, a UTC-PD chip, a hemispherical Si lens, and an optical fibre with optical lens. The slot antenna and coplanar waveguide (CPW) were formed on an Si substrate. A UTC-PD chip was flip-chip bonded on the CPW pads. Optical signals delivered with an optical fibre cable are focused onto the UTC-PD. The resulting electrical signals travel along the CPW to the slot antenna. This produces MMW signals, which are collimated by the hemispherical lens and radiated into free space.

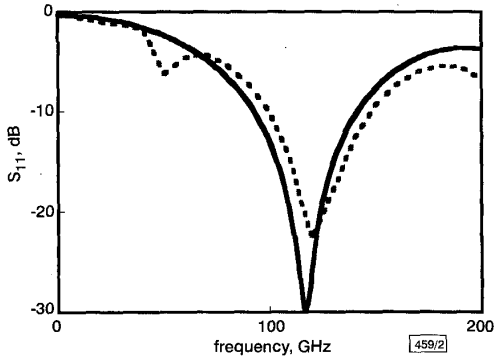

Fig. 2 *Simulation and measurement results of S_{11}*

——— measurement
– – – – simulation

We designed a CPW-fed slot antenna that operates at 120 GHz by a three-dimensional electromagnetic field simulator using a finite-element method. The slot length (L) is 774 μm and the slot width (W) is 95 μm. The accuracy of the simulator has been verified by comparing simulation with the measurement results obtained by an ONA. The measurement and simulation results of input reflection coefficient S_{11} are shown in Fig. 2. The resonant frequency that is determined by simulation and measurement is 120 and 117 GHz, respectively. Thus, simulated and measured responses agreed well, and the effectiveness of the simulators over 100 GHz frequency was confirmed.

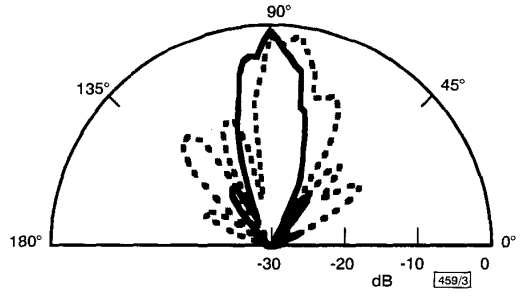

Fig. 3 *Radiation patterns of photonic transmitter*

——— H-plane
– – – – E-plane

Measurement results: In the experiment, a 120 GHz optical signal is made by multiplexing 60 GHz repetitive frequency pulse trains generated from a modelocked laser diode integrated with an electro-absorption modulator [5]. The 3 dB bandwidth of the UTC-PD used was about 100 GHz. Fig. 3 shows the radiation patterns of the photonic transmitter. The radiated power is collimated along an axis almost perpendicular to the substrate, which indicates that the Si lens works very well.

Next, we measured the radiated output power of the photonic transmitter. The radiated power from the transmitter was collimated and focused on the horn antenna by two Teflon lenses. The received MMW power was measured by a waveguide-mounted detector using Schottky diodes.

Fig. 4 shows the dependence of the detected power on the photocurrent. The detected power is found to first increase almost linearly with the photocurrent, then tending to saturate. This comes from the nonlinear saturation of UTC-PD at frequencies beyond its 3 dB bandwidth. The maximum detected power was 0.25 mW. To our knowledge, this is the first time that the MMW power emitted into free space from a PD-integrated antenna was detected at a frequency > 100 GHz.

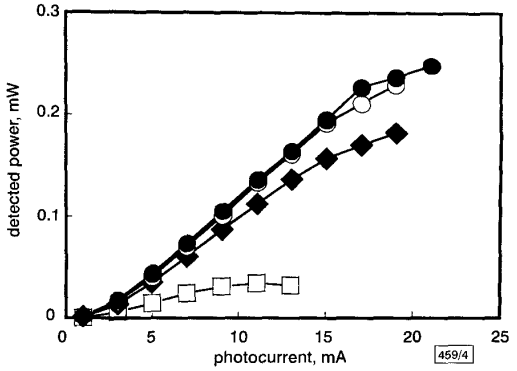

Fig. 4 *Detected MMW power of photonic transmitter*

—●— bias voltage = 3 V
—○— bias voltage = 2 V
—◆— bias voltage = 1 V
—□— bias voltage = 0 V

Conclusion: A 120 GHz slot antenna has been designed and tested successfully. It was integrated with a UTC-PD and a hemispherical Si lens to form a compact MMW transmitter. The detected output power of the transmitter exceeded 0.2 mW, which is the highest value ever reported for > 100 GHz photonic transmitter.

26 January 2001
Electronics Letters Online No: 20010968
DOI: 10.1049/el:20010968

A. Hirata and T. Nagatsuma (*NTT Telecommunications Energy Laboratories, 3-1, Morinosato Wakamiya, Atsugi-shi, Kanagawa Pref., 243-0198, Japan*)

E-mail: ahirata@aecl.ntt.co.jp

References

1 CHAKAM, G.A., and FREUDE, W.: 'Coplanar phased array antenna with optical feeder and photonic bandgap structure'. Tech. Dig. MWP'99, Melbourne, 1999, Post-Deadline Session, pp. 1–4

2 TAKAHATA, K., MURAMOTO, Y., FUKUSHIMA, S., FURUTA, T., and ITO, H.: 'Monolithically integrated millimeter-wave photonic emitter for 60-GHz fiber-radio application'. Tech. Dig. MWP 2000, Oxford, 2000, pp. 229–323

3 SAHRI, N., and NAGATSUMA, T.: 'Packaged photonic probes for an on-wafer broad-band millimeter-wave network analyzer', *Photonics Technol. Lett.*, 2000, **12**, pp. 1225–1227

4 ISHIBASHI, T., SHIMIZU, N., KODAMA, S., ITO, H., NAGATSUMA, T., and FURUTA, T.: 'Uni-traveling-carrier photodiodes', *Tech. Dig. Ultrafast Electron. and Optoelectron.*, 1997, pp. 166–169

5 NAGATSUMA, T., SAHRI, N., YAITA, M., ISHIBASHI, T., SHIMIZU, N., and SATO, K.: 'All optoelectronic generation and detection of millimeter-wave signals'. Tech. Dig. MWP'98, New Jersey, 1998, pp. 5–8

Continuous-wave THz imaging

T. Kleine-Ostmann, P. Knobloch, M. Koch, S. Hoffmann, M. Breede, M. Hofmann, G. Hein, K. Pierz, M. Sperling and K. Donhuijsen

The first THz imaging spectrometer based on continuous-wave THz radiation is presented. The new setup is less expensive and more compact than conventional time-domain imaging systems that comprise femtosecond lasers instead. As an example we investigate a human liver with metastasis.

Introduction: The spectral range between a few hundred gigahertz and several terahertz (THz) was traditionally hard to access. Recently THz imaging was demonstrated using pulsed THz radiation generated by femtosecond laser pulses and photoconductive dipole antennas [1] or nonlinear crystals [2]. Currently the poten-

tial of THz imaging which yields a better resolution than microwave imaging [3] is extensively studied, in particular for biomedical applications.

At present, research focuses on the application of continuous-wave (CW) THz radiation [4] for imaging purposes [5]. In contrast to the well established time-domain spectroscopy based on femtosecond THz pulses, CW imaging has the advantage of a much higher spectral power density at the desired frequency because the power of the THz pulse is distributed over its entire spectral width. Since the spectral resolution of a CW THz imaging system depends merely on the frequency stability of the two laser modes involved in photomixing, a higher frequency resolution can be achieved than with a conventional pulsed THz radiation setup. Instead, time-domain imaging in a distinct narrow frequency interval requires a time-consuming increase of scanning range and resolution together with additional efforts for Fourier transform and spectral integration. Still time-domain systems do not offer the prospective signal-to-noise ratio of a much faster and simpler CW system.

A first attempt towards the development of CW imaging based on THz generation by mixing of two laser frequencies in photoconducting antennas has been made by Siebert *et al.* [5]. For this purpose they developed a two-colour Ti:sapphire laser, pumped by an argon-ion laser. Its tuning capability ranges from 1 GHz up to 50 THz at 250 mW output power in both modes. The excellent performance of this laser makes it a promising light source for future photomixing applications. However, the laser source appears to be expensive and requires a complex laboratory setup.

In this Letter we present a CW imaging system that uses a two-colour external-cavity laser diode instead [6]. Hence it is much less expensive and more compact as compared to systems based on optically pumped solid-state lasers. As an example we present a first CW THz transmission image of a human liver which contains cancerous tissue.

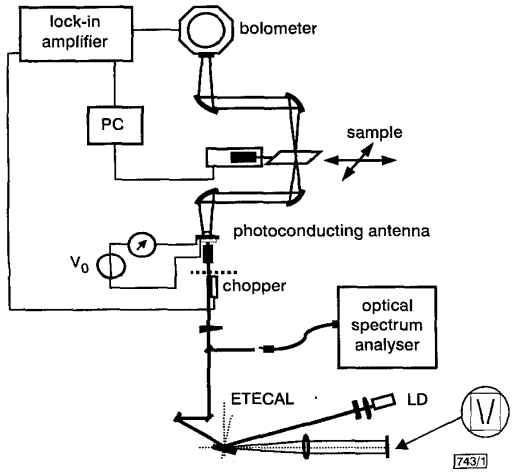

Fig. 1 *Setup of continuous-wave THz imaging system including two-mode external cavity laser diode (ETECAL), photomixer and bolometer*

Sample is scanned in intermediate focus of THz radiation

Experimental setup: Our CW THz imaging setup, which is shown in Fig. 1, uses the electronically tunable external-cavity laser diode (ETECAL) [6] as a light source. To facilitate the measurements a V-shaped mirror instead of an electronically tunable liquid crystal array serves as the frequency selective element. The frequency spacing of the two laser modes can be adjusted by moving the V-mirror vertically and is set to 230 GHz which is the resonance frequency of the photoconducting dipole antenna used for photomixing. The two-line laser emission with a total optical power of 29 mW is focused onto the 5 μm wide gap of a 50 V DC-biased stripline dipole antenna. The dipole has a length of 400 μm and was deposited on a low temperature grown (LT) GaAs substrate. The epitaxial layer was grown at 300°C and annealed at 600°C for 10 min to achieve short carrier lifetimes in the ps range which are necessary for photomixing. For detection of the THz radiation a standard bolometer is used. Four off-axis parabolic mirrors allow us to obtain an intermediate focus of the THz waves. To accumulate an image of the THz transmittivity of an object, the sample is simply translated through the focus and a PC is used to acquire the detected signal pixel by pixel using the lock-in technique.

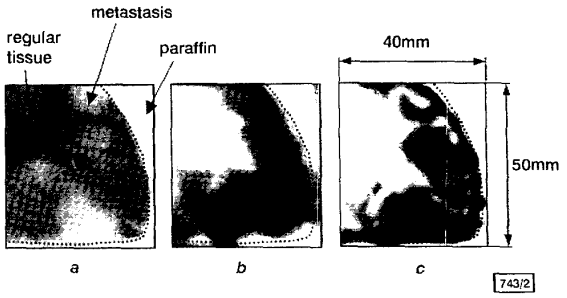

Fig. 2 *Images of liver sample with tumours*

a Optical image
b THz transmission image at 230 GHz using CW radiation (interpolated to contour lines)
c THz transmission image for frequency window from 0.2 to 0.5 THz using pulsed radiation (interpolated to contour lines)

Sample: To demonstrate CW THz imaging we examine the transmission properties of a human liver with several tumours that has undergone the standard procedure for histo-pathological investigation [7]. To fix the protein structure it was put in a formalin solution for several hours, then subjected to a series of alcohols and finally to xylol to remove the water. After that it was embedded in paraffin and manually cut into a 50 × 40 × 4 mm block. In the optical image, which can be seen in Fig. 2*a*, the cancerous areas are somewhat brighter than the regular tissue.

Results and discussion: Fig. 2*b* shows a CW THz image of the sample acquired at a frequency of 230 GHz and scanned with 0.5 mm stepsize of the translation stage. The tumours appear as dark patches of reduced transmission and are clearly distinguishable from regular tissue. While areas of paraffin and regular tissue exhibit a maximum transmission of ~60% (freespace transmission set to 100%), the transmission of the cancerous regions decreases down to values of 18%. The level of detail is not yet as good as that of a previously measured transmission image shown in Fig. 2*c* using pulsed THz radiation and an integration window from 0.2 to 0.5 THz, which turned out to provide the best contrast [7]. The CW frequency of 230 GHz, located at the lower end of the integration interval used for the pulsed THz radiation image, is responsible for a reduced spatial resolution. In addition, in this first demonstration the signal-to-noise ratio was only 75 which also diminishes the quality of the image. Currently we are working towards an improved signal-to-noise ratio by optimising the LT-GaAs emitter antennas.

The question arises whether the structural differences in THz absorption are due to variations in the density or in the chemical composition of the tissue. However, since the density is supposed to be rather similar for metastasis and regular tissue, we suspect that the contrast is due to different chemical properties of the tissue. Further investigations to clarify this point are under way.

Conclusion: We have demonstrated the first CW THz imaging system. This was accomplished using a two-colour diode laser which is much less expensive and considerably more compact than femtosecond laser systems which are widely used for conventional pulsed THz imaging and also other laser sources considered for CW THz generation. We presented a first CW THz image of a human liver with metastasis. Cancerous and regular tissue can be distinguished. We suspect that CW radiation has a high potential for many imaging applications since it is possible to obtain low-noise transmission images at precisely defined frequencies. By tuning the CW frequency to the respective absorption line, it should even be possible to visualise distinct subtances.

Acknowledgments: We thank H. Niemann and B. Güttler of the Physikalisch-Technische Bundesanstalt for technical assistance.

17 September 2001
Electronics Letters Online No: 20011003
DOI: 10.1049/el:20011003

T. Kleine-Ostmann, P. Knobloch and M. Koch (*Institut für Hochfrequenztechnik, Technische Universität Braunschweig, Schleinitzstraße 22, 38106 Braunschweig, Germany*)

S. Hoffmann, M. Breede and M. Hofmann (*Fachbereich Physik und Wissenschaftliches Zentrum für Materialwissenschaften, Philipps-Universität Marburg, Renthof 5, 35032 Marburg, Germany*)

G. Hein and K. Pierz (*Physikalisch-Technische Bundesanstalt, Bundesallee 100, 38116 Braunschweig, Germany*)

M. Sperling and K. Donhuijsen (*Institut für Pathologie, Städtisches Klinikum, Celler Straße 38, 38114 Braunschweig, Germany*)

References

1 MITTLEMAN, D.M., GUPTA, M., NEELAMANI, R., BARANIUK, R.G., RUDD, J.V., and KOCH, M.: 'Recent advances in THz imaging', *Appl. Phys. B*, 1999, **68**, pp. 1085–1094

2 HAN, P.Y., CHO, G.C., and ZHANG, X.-C.: 'Time-domain transillumination of biological tissues with terahertz pulses', *Opt. Lett.*, 2000, **25**, (4), pp. 242–244

3 TOFIGHI, M.-R., and DARYOUSH, A.S.: 'Near field microwave brain imaging', *Electron. Lett.*, 2001, **37**, (13), pp. 807–808

4 BROWN, E.R., McINTOSH, K.A., NICHOLS, K.B., and DENNIS, C.L.: 'Photomixing up to 3.8 THz in low-temperature-grown GaAs', *Appl. Phys. Lett.*, 1995, **66**, (3), pp. 285–287

5 SIEBERT, K.J., QUAST, H., and ROSKOS, H.G.: 'Perspectives of continuous-wave optoelectronic THz imaging' *in* MILES, R.E., *et al.* (Eds.): 'Terahertz sources and systems' (Kluwer Academic Publishers, 2001)

6 STRUCKMEIER, J., EUTENEUER, A., SMARSLY, B., BREEDE, M., BORN, M., HOFMANN, M., HILDEBRAND, L., and SACHER, J.: 'Electronically tunable external-cavity laser diode', *Opt. Lett.*, 1999, **24**, (22), pp. 1573–1574

7 KNOBLOCH, P., SCHMALSTIEG, K., KOCH, M., REHBERG, E., VAUTI, F., and DONHUIJSEN, K.: 'THz imaging of histo-pathological samples'. European Conferences of Biomedical Optics (ECBO), Munich, June 2001

Generation of micro- and THz-waves at 1.5 μm by dual-frequency Er:Yb laser

S. Taccheo, G. Sorbello, G. Della Valle, P. Laporta, G. Karlsson, F. Laurell, W. Margulis and S. Cattaneo

A promising technique for generating discrete-tunable beat-note signals is presented and investigated. Two tunable fibre gratings provide external feedback to an Er:Yb laser. Beat-notes from 60 GHz up to ~2 THz are achieved. Power equalisation is discussed and the partition noise is measured.

Introduction: Delivery of microwave signals on optical carriers is a promising evolution of microwave networks [1]. In addition, sources of high-frequency signals (hundreds of gigahertz up to several terahertz) are interesting for many applications from far infrared spectroscopy [2] to optical communications [3]. An effective technique to generate microwave and THz-signals is to use the beat-note of two continuous wavelength signals generated from a dual wavelength laser source. Several dual-wavelength laser sources have been proposed so far, both semiconductor lasers [4, 5] and bulk lasers with separated intracavity-beam paths [6].

In this Letter we describe a straightforward and promising alternative technique for generating microwave and THz signals based on a compound cavity formed by a standard multi-wavelength laser cavity with external feedback provided by two fibre Bragg gratings (FBG). This source joins the high-temporal coherence of a solid-state laser with the simplicity of FBG tuning. We also investigate the properties and limitation of such approach.

Laser setup: Fig. 1 shows the dual-frequency laser cavity setup. The laser source is a double cavity consisting of a main cavity (dashed box in Fig. 1) and two external FBGs. The main cavity is a standard diode-pumped bulk Er:Yb:phosphate glass laser [7] consisting of two elements: a 1 mm thick plano-plano Er:Yb glass rod and a 10 mm radius of curvature 98% reflectivity output coupler. The main cavity is therefore a multi-wavelength oscillator with high-finesse and high-free spectral range (FSR ~15–30 GHz); the free running wavelengths are all at around the erbium gain peak at ~1533 nm. The main difference with respect to previous reported cavities is the pumping system. To reduce the size of the laser device, we used only a single GRIN lens (dot pitch 0.28) to focus the radiation emitted by a broad area (1 × 100 μm²) InGaAs laser diode. However the GRIN lens cannot compensate for the strong ellipticity of the pump laser diode and the maximum pump power was limited by thermal effects to a value of ~300 mW. Note that the ytterbium concentration was similar to [7] and a QX glass base (Kigre Inc.) has been used to reduce thermal stress. The maximum output power was ~45 mW at 1533 nm with 70 mW pump power threshold in multimode operation. The output coupler was glued to a piezoelectric transducer (PZT) for fine tuning of the main cavity FSR. The output beam from the main cavity was focused into a singlemode fibre by suitable optics with efficiency greater than 80%.

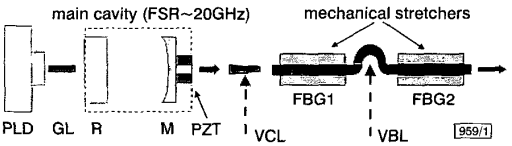

Fig. 1 *Schematic diagram of laser cavity*

PLD: pump laser diode; GL: grin lens; R: laser rod; M: R = 98% mirror; PZT: piezoelectric transducer; LS: lens system; VBL: variable (macro)bending losses; VCL: variable coupling losses

To achieve dual-frequency operation we used external feedback provided by two cascaded FBG gratings as shown in Fig. 1. The FBG peak wavelengths define the two oscillating wavelengths provided that their reflectivity is properly chosen. In our experimental setup, unless otherwise stated, we used two 1550.4 nm centre wavelength FBGs acting as output coupler of the compound cavity. The FBGs full-width half maximum (FWHM) was ~33 GHz and the reflectivity was 80% and 90% for FBG1 and FBG2, respectively, the FBG2 reflectivity being larger to compensate for the extra splicing fibre loss. In this configuration we observed that the free-running lasing at 1533 nm was suppressed in favour of lasing at the FGB centre wavelength (1550.4 nm) when ~50% of the main cavity output power was coupled into the fibre.

A mechanical stretcher was able to provide up to ~3 nm tuning for gratings. The beat-note tuning was carried out by mechanical stretching of the FBG and optimised by matching the main cavity FSR to the new FBG peaks by finetuning the PZT. The advantage of the present system, compared to other dual-wavelength bulk lasers with independent intracavity beam paths, is that the main cavity never needs realigning and therefore the tuning process is very reliable despite the limitation arising from the need to match both FBGs' peaks and main cavity FSR. The linewidth of each mode was below 10 kHz and the relative short-term mode-spacing stability ($\Delta\nu/\nu$) was better than 10^{-7}.

The main issue for dual-frequency lasers is power equalisation in order to avoid a bias continuous-wave signal superimposed to the beat-note. We achieve power equalisation by using two different techniques depending on the frequency separation. If the frequencies are close (< a few hundred gigahertz) we introduced extra loss in the second FBG cavity by, for example, tuning the fibre macrobending loss. When the frequencies are far apart (> ~8 nm, i.e. they operate on different Stark transitions) finetuning of the common cavity loss by changing the main cavity to fibre coupling efficiency is able to equalise the power of the two wavelengths [8].

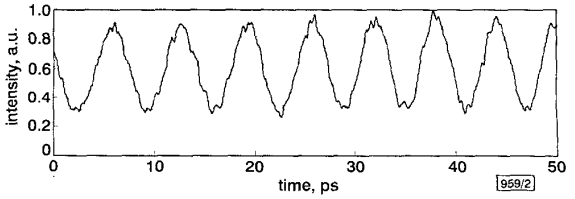

Fig. 2 *160 GHz beat-note autocorrelation trace*